EurJIC
European Journal of Inorganic Chemistry

Full Paper
doi.org/10.1002/ejic.202000681

Lutidine-Derived Ligands

Metalated Ir–CNP Complexes Containing Imidazolin-2-ylidene and Imidazolidin-2-ylidene Donors – Synthesis, Structure, Luminescence, and Metal–Ligand Cooperative Reactivity

Martín Hernández-Juárez,[a,b] Práxedes Sánchez,[a] Joaquín López-Serrano,*[a] Patricia Lara,[a] Pablo González-Herrero,*[c] Nuria Rendón,[a] Eleuterio Álvarez,[a] Margarita Paneque,[a] and Andrés Suárez*[a]

Abstract: The iridium complex **1** based on a metalated CNP ligand containing an imidazolin-2-ylidene fragment has been prepared by treatment of the ligand precursor **4** with Ag_2O followed by reaction with $[IrCl(COE)_2]_2$. The chlorohydride imidazolidin-2-ylidene complex **6**, which is isostructural to **1**, was synthetized by reaction of the previously reported dihydride derivative **3** with CH_2Cl_2. Complexes **1** and **6** exhibit luminescence arising from a ^{3}MLCT/ILCT state involving the metalated CNP ligand, which is particularly intense for **1** in the solid state at 298 K. Furthermore, the reactivity of complexes **1** and **6** towards bases was compared. Deprotonation of **1** with KO*t*Bu produced the selective formation of the dinuclear complex **7**; meanwhile, the reaction of **6** led to a complex mixture of products. The same reactions carried out in the presence of PPh_3 produced the selective deprotonation of the P-bonded methylene bridges of **1** and **6**, yielding the isostructural derivatives **9** and **10**. DFT calculations performed on the *u*NHC-containing tautomers **I** and **II**, and the *s*NHC-based isomers **III** and **IV**, showed that the NHC-deprotonated derivatives **II** and **IV** are more stable by 3.20 and 2.73 kcal mol^{-1}, respectively, than their P-deprotonated counterparts (**I** and **III**). However, a reverse stability order was observed for hexacoordinated tautomers **I·L** and **II·L**, and **III·L** and **IV·L** (L = PPh_3, CO, MeCN). Finally, the catalytic activity of complex **3** in the transfer hydrogenation of ketones has been assessed.

Introduction

The study of metal complexes capable of metal–ligand cooperation has become a pivotal aspect to the development of new stoichiometric and catalytic processes.[1,2] Among the proton-responsive ligand-metal systems, derivatives based on lutidine-derived pincer ligands have received a special attention due to their ability to promote ligand-assisted substrate activation triggered by the reversible deprotonation of the methylene arms of the ligand and concomitant dearomatization of the central pyridine ring.[2] While development of these systems has been mainly associated to PNX (P = bulky electron-rich phosphane, X = phosphane or hemilabile N-donor) pincers (Figure 1),[2,3] structural variations involving the substitution of the side PR_2 groups by other strong σ-donors, such as N-heterocyclic carbenes (NHC), should have an effect on both the elec-

[a] *Dr. M. Hernández-Juárez, Dr. P. Sánchez, Dr. J. López-Serrano, Dr. P. Lara, Dr. N. Rendón, Dr. E. Álvarez, Prof. M. Paneque, Dr. A. Suárez*
Instituto de Investigaciones Químicas (IIQ), Departamento de Química Inorgánica and Centro de Innovación en Química Avanzada (ORFEO-CINQA), CSIC and Universidad de Sevilla,
Sevilla 41092, Spain
E-mail: joaquin.lopez@iiq.csic.es
andres.suarez@iiq.csic.es
https://osaca.iiq.us-csic.es/
[b] *Dr. M. Hernández-Juárez*
Área Académica de Química, Centro de Investigaciones Químicas, Universidad Autónoma del Estado de Hidalgo (UAEH),
Km. 14.5 Carretera Pachuca-Tulancingo, Ciudad del Conocimiento, C.P. 42184, Mineral de la Reforma, Hidalgo, Mexico
[c] *Dr. P. González-Herrero*
Departamento de Química Inorgánica, Facultad de Química, Universidad de Murcia,
Murcia 30071, Spain
E-mail: pgh@um.es
Supporting information and ORCID(s) from the author(s) for this article are available on the WWW under https://doi.org/10.1002/ejic.202000681.

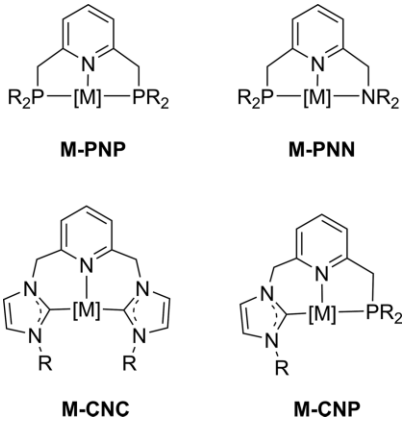

Figure 1. General structures of metal complexes with lutidine-derived PNP, PNN, CNC and CNP ligands.

Full Paper
doi.org/10.1002/ejic.202000681

tronic and steric properties of the complexes, and lead to significant differences in their reactivity.

Imidazolin-2-ylidenes (*u*NHC, Figure 2) and imidazolidin-2-ylidenes (*s*NHC), two important classes of N-heterocyclic carbenes,[4] are nowadays amply employed spectator ligands in prominent homogeneous catalytic reactions, including C–C and C–X couplings,[5] olefin metathesis[6] and hydrogenations,[7] due to their substantial structural diversity and excellent σ-donor characteristics.[4] The stereoelectronic properties of imidazolin-2-ylidenes and imidazolidin-2-ylidenes are relatively similar,[8] as shown by the slightly lower Tolman Electronic Parameter (TEP) values and larger buried volumes of *s*NHCs in comparison to their *u*NHC counterparts. However, the metal–NHC bonding of *u*NHCs and *s*NHCs is significantly different since, although both are strong σ-donors, in electron-rich metal complexes imidazolidin-2-ylidenes are also able to accept significant π-backdonation.[8,9] These electronic differences have a profound impact on both the stoichiometric and catalytic reactivity of metal–NHC complexes.[6,10]

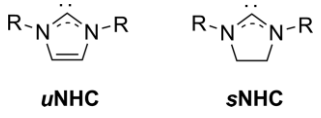

Figure 2. General structures of imidazolin-2-ylidene (*u*NHC) and imidazolidin-2-ylidene (*s*NHC) ligands.

Unsurprisingly, several groups have studied the coordination properties and reactivity of metal complexes based on NHC-containing lutidine-based CNX pincers (C = imidazolin-2-ylidene, X = imidazolin-2-ylidene or hemilabile N-donor), as well as their applications in catalytic reactions.[11–17] Deprotonation of the methylene CH_2-*u*NHC arms of these derivatives lead to species that are able to participate in ligand-assisted processes. Moreover, since 6-membered chelates are formed upon coordination of the Py–CH_2–*u*NHC linkage, replacement of phosphane donors by *u*NHCs not only affects the electronic properties of the complexes, but also confers a greater flexibility to the ligand in comparison to the 5-membered rings formed with PNX pincers. This larger flexibility imparted by the presence of the *u*NHC donors in lutidine-based CNX pincer ligands allows to stabilize metal complexes in a variety of coordination geometries, what is an important feature in a catalytic process since reaction intermediates might need to adopt different coordination environments. For example, while PNP ligands only exhibit meridional coordination modes, facial coordination of CNC ligands in Ru complexes has been observed.[17] More remarkable, however, is the fact that the larger chelate ring of the CNC pincer complexes might result in enhanced reactivities, as shown by the Pidko's group in the reactions of deprotonated Ru–CNC systems towards H_2 and CO_2.[13]

Recently, some of us reported new iridium complexes stabilized by ligands having *u*NHC and phosphane side donors and a lutidine central fragment (CNP, Figure 1), and assessed their ability to adapt to different coordination geometries and participate in the ligand-assisted activation of H_2.[18,19] These non-symmetric pincer ligands permit the tuning of two different side donors, thus allowing a larger electronic and steric diversity,[20] and serve for a direct comparison of the properties of the *u*NHC- and phosphane-containing halves of the pincer. Furthermore, we have communicated the selective hydrogenation of the olefinic backbone of a coordinated imidazolin-2-ylidene fragment that occurs in an iridium complex based on a metalated κ^4-(P,N,C^{uNHC},C^{aryl}) lutidine-derived ligand.[21] It is worth noting that, with few notable exceptions, the reactivity of the –HC=CH– backbone of coordinated imidazolin-2-ylidenes has been scarcely explored.[22] The reaction of complex **1** with H_2 in the presence of base (KO*t*Bu) initially yielded the dihydride complex **2**, involving a ligand-assisted H–H activation (Scheme 1). Upon prolonged exposure to H_2, complex **2** was hydrogenated at the imidazolin-2-ylidene –CH=CH– moiety leading to the imidazolidin-2-ylidene dihydride derivative **3**. In contrast to complex **2**, which is only stable under H_2, the dihydride **3** was readily isolated as an air-stable solid. This difference is expected to arise from the presence of a better electron-donating imidazolidin-2-ylidene fragment in **3**.

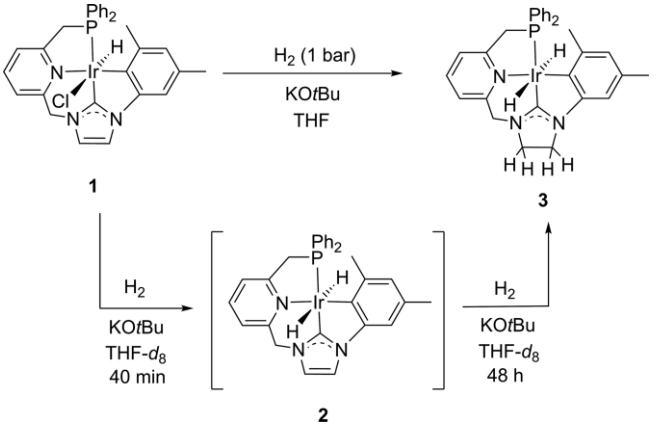

Scheme 1. Hydrogenation of complex **1** to yield **2** and **3**.

To get further insight into the effect of substituting a *u*NHC donor by a *s*NHC fragment, we deemed interesting to expand our investigations on these metalated iridium complexes containing κ^4-(P,N,C^{NHC},C^{aryl}) ligands. These include a detailed study of their structural features and photophysical properties, as well as a comparison of the acid-base reactivity of the CH_2–P, CH_2–*u*NHC and CH_2–*s*NHC methylene bridges of the ligands and their participation in ligand assisted processes.

Results and Discussion

Synthesis and Structure of Metalated Ir–CNP Complexes

Treatment of the imidazolium salt **4** with Ag_2O in CH_2Cl_2 followed by reaction with $[IrCl(COE)_2]_2$ in a **4**/Ir = 1:1 ratio resulted in the expected coordination of the lutidine-derived CNP pincer ligand accompanied of the activation of the *ortho* C–H bond of the xylyl fragment,[23] thus allowing the isolation of complex **1** (Scheme 2). The synthesis of **1** has been previously accomplished by the prolonged heating of a toluene suspension of the diolefin complex **5**.[21]

Full Paper
doi.org/10.1002/ejic.202000681

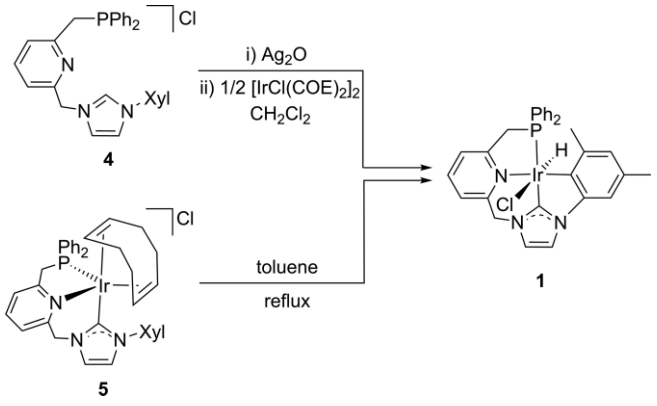

Scheme 2. Synthesis of complex **1**.

As reported, complex **1** reacts with H_2 (1–2 bar) in the presence of KO*t*Bu (1 equiv.) producing the initial formation of the imidazolin-2-ylidene dihydride derivative **2**, which upon standing under a H_2 atmosphere for 48 h is transformed to the dihydride Ir derivative **3** that features an imidazolidin-2-ylidene ligand fragment (Scheme 1).[21] Reaction of **3** with CH_2Cl_2 yielded the chlorohydride derivative **6** (Scheme 3), which has been fully characterized. The ^{1}H NMR spectrum in CD_2Cl_2 of **6** shows a doublet hydride signal at δ = –22.26 ($^2J_{HP}$ = 16.0 Hz); whereas in the ^{13}C{^{1}H} NMR experiment the carbene carbon produces a doublet resonance at 203.9 ppm (J_{CP} = 113 Hz). As expected from the comparison of the NMR properties of metal complexes containing saturated and unsaturated NHCs, in the ^{13}C{^{1}H} NMR spectrum, the latter signal is significantly shifted downfield with respect to the same resonance of the complex [IrH(PNC^{uNHC}C^{aryl})(MeCN)]BF_4 (δ_C = 172.3; d, J_{CP} = 108 Hz),[24] an analogue soluble version of complex **1**.[21]

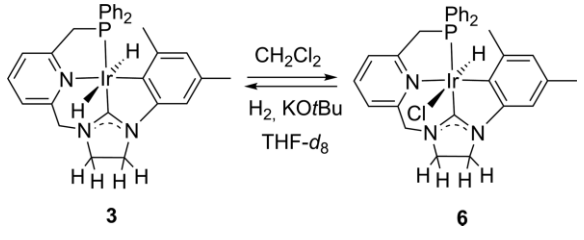

Scheme 3. Synthesis of complexes **3** and **6**.

The structure of **6** was studied by single-crystal X-ray diffraction techniques (Figure 3). Although complex **6** in the solid state exhibits very similar features to complex **1**, the tetradentate ligand adopts a slightly less planar structure than in **1**,[21] as reflected in the values of the torsion angles of the chelates involving the pyridine moiety with the phosphane and *s*NHC donors [C(17)–N(3)–Ir(1)–P(1) = –22.9(4)°; C(13)–N(3)–Ir(1)–C(1) = –11.2(5)°]. Moreover, as expected, a significantly elongated C–C distance of 1.521(9) Å in the carbene moiety with respect to complex **1** [1.348(4) Å] is found, as well as a small but significant widening of the N–C–N angle [N(1)–C(1)–N(2) = 109.4(6)°, **6**; 106.8(2)°, **1**].[8] Furthermore, the *s*NHC ring has a planar configuration, albeit a significantly larger torsion angle N(1)–C(3)–C(2)–N(2) of 4.5(6)° in comparison to **1** [0.3(3)°] is observed, as expected from the disruption of the π-electron delocalization between the NCN and C–C units of the imidazolidin-2-ylidene.[25] Finally, it is worth mentioning that the carbene NCN moiety remains coplanar to the arene fragment, as indicated by the C(1)–N(1)–C(4)–C(5) dihedral angle of 0.6(8)°.

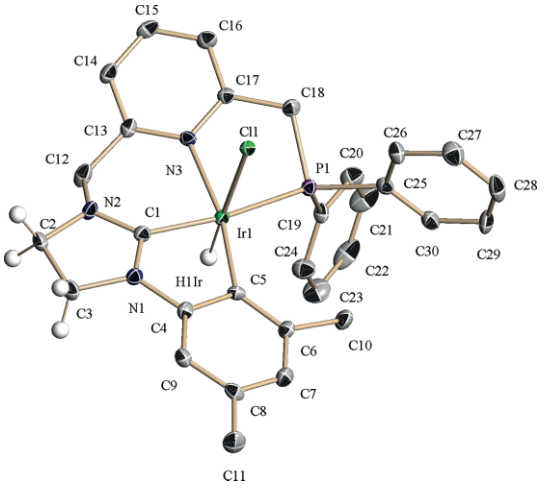

Figure 3. ORTEP drawing at 30 % ellipsoid probability of complex **6**. Hydrogen atoms, except hydrido ligands and the *s*NHC hydrogens, have been omitted for clarity. Ir(1)–C(1) 1.955(6), Ir(1)–N(3) 2.163(5), Ir(1)–P(1) 2.3408(15), Ir(1)–Cl(1) 2.5452(15), Ir(1)–C(5) 2.081(6), C(1)–Ir(1)–P(1) 170.4(2), C(1)–Ir(1)–C(5) 78.0(3), C(1)–Ir(1)–N(3) 89.5(2), P(1)–Ir(1)–N(3) 81.33(13).

As shown with complex **1**, derivative **6** cleanly reacted with H_2 in the presence of KO*t*Bu to yield the dihydride derivative **3**, likely involving a ligand-assisted H–H activation (Scheme 3).

Photophysical Properties of 1 and 6

Solid samples of complexes **1** and **6** display significant luminescence at room temperature, which motivated us to carry out a complete photophysical study.[26,27] Both complexes show a broad band at around 390 nm as the lowest-energy feature in the UV/Vis absorption spectra (Table 1 and Figure S8). On the basis of its solvatochromic behavior (Figure S9),[28] relatively low molar extinction coefficients and lack of vibrational structure, we assign the corresponding transition as having a marked metal-to-ligand charge-transfer (MLCT) character. Further insight into its nature was gained from DFT and TDDFT calculations on complex **1** (see Supporting Information). The HOMO in this complex is a combination of π orbitals of the aryl–NHC fragment of the ligand with d(Ir) and p(Cl) orbitals, while the LUMO is a π* orbital of the pyridine fragment (Figure S15). The lowest-energy singlet excitation, predicted at 424 nm in CH_2Cl_2 solution, corresponds to a HOMO-LUMO transition, and can be therefore described as an admixture of metal-to-ligand and intraligand charge transfer (MLCT/ILCT) with some ligand-to-ligand charge-transfer (LLCT) character due to the involvement of p(Cl) orbitals.

Table 1. Electronic absorption data of **1** and **6** in CH_2Cl_2 solution at 298 K.

Complex	λ [nm] (ε [M^{-1} cm^{-1}])
1	289 (sh, 5300), 336 (sh, 2200), 393 (2500)
6	289 (sh, 9300), 391 (2700)

Full Paper
doi.org/10.1002/ejic.202000681

The emission data of **1** and **6** are summarized in Table 2. Complex **1** displays strong emission in the solid state at 298 K, while complex **6** is a very weak emitter. In all cases the emissions are broad and do not show vibrational structure, which agree with a significant MLCT contribution to the emitting state. None of the studied complexes emits appreciably in fluid solutions at 298 K and therefore their emissions were examined in 2-methyltetrahydrofuran (MeTHF) frozen glasses at 77 K (Figure 4). The excitation profiles consistently reproduce the lowest-energy charge-transfer band observed in the absorption spectra. The emission lifetimes are consistent with an emitting state of triplet parentage and high MLCT character.[29] The TDDFT calculations on **1** show that the lowest-energy vertical triplet excitation corresponds to a HOMO–LUMO transition and therefore the emitting excited state in these complexes probably has a similar orbital nature.

Table 2. Emission data of complexes **1** and **6**.

	Medium	λ_{exc} [nm][a]	λ_{em} [nm]	τ [μs][b]	Φ[c]
1	Solid, 298 K	*366*, 448	506	2.1 (13 %), 6.3 (87 %)	0.281
	MeTHF, 77 K	*300*, 336, 391	492	21 (62 %), 53 (38 %)	–
6	Solid, 298 K	*364*, 416	517	0.21 (10 %), 0.93 (90 %)	< 0.01[d]
	MeTHF, 77 K	*289*, 383	486	30 (28 %), 62 (72 %)	–

[a] The most intense peak is italicized. [b] Emission lifetime; biexponential decays were observed; relative amplitudes are given in parentheses. [c] Absolute quantum yield. [d] Could not be measured accurately.

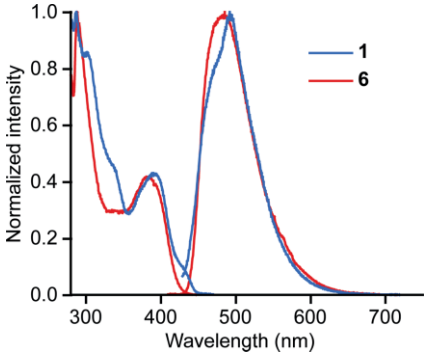

Figure 4. Excitation (left) and emission (right) spectra of **1** and **6** in MeTHF frozen glasses at 77 K.

Deprotonation of Complexes 1 and 6

The acid-base properties of the methylene bridges of lutidine-derived ligands are of relevance to the development of processes involving metal–ligand cooperation.[2] Reactions of complexes **1** and **6** with H_2 in the presence of KO*t*Bu produced the dihydride complexes **2** and **3**, respectively, whose formation is assumed to involve a ligand-assisted process. Since these Ir–CNP complexes contain two non-equivalent methylene pincer arms, they are suitable systems to compare the acid-base reactivity of the CH_2P arm with that of both CH_2–*u*NHC and CH_2–*s*NHC pincer bridges. Previously, the reactivity of ruthenium complexes incorporating unsymmetrical PNN and CNN ligands towards bases has been investigated.[14,30]

As previously communicated, reaction of **1** with KO*t*Bu in THF yielded the poorly soluble bimetallic species **7** (Scheme 4).[21] Formation of this derivative was also observed upon removal of the H_2 atmosphere from pressurized solutions of **2**. Complex **7** possesses a dinuclear structure, in which the two iridium centers are bonded to the opposite ligands through the CH-*u*NHC bridges, and the metalated CNP ligands have a rather planar conformation. Formation of **7** might involve the initial deprotonation of the CH_2N arm of **1**, and a subsequent dimerization of the resulting species facilitated by the planarity of the deprotonated Ir–CNP units.[31,32] The Pidko group and some of us, independently, have previously noted that picolyl-NHC fragments of Ru–CNC complexes are readily deprotonated upon reaction with base, and the resulting species are prone to react with electrophiles.[12,13,17]

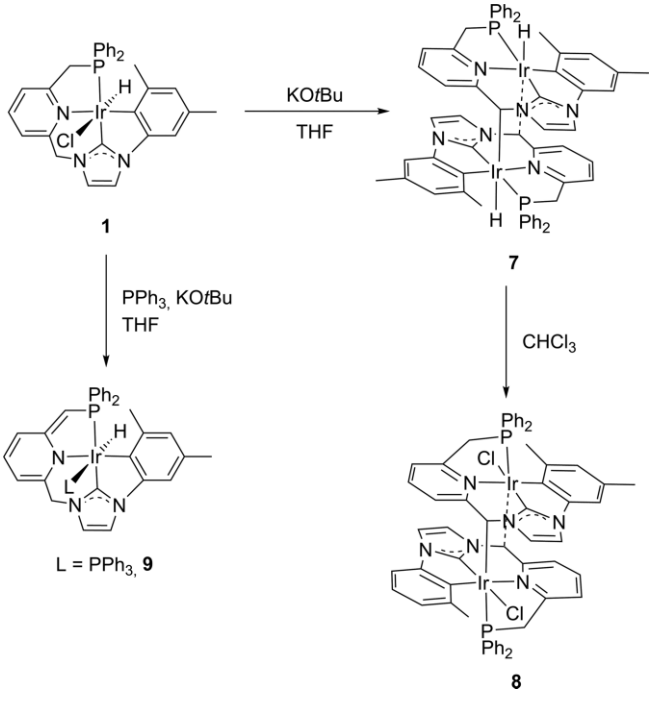

Scheme 4. Synthesis of complexes **7**–**9**.

Subsequent treatment of **7** with $CHCl_3$ gave rise to the highly insoluble chloro complex **8** (Scheme 4). Crystals adequate for an X-ray diffraction study of the dinuclear derivative **8** were obtained from saturated THF solutions (Figure 5). The iridium atoms of **8** have an octahedral coordination geometry, however at variance with complex **7**, the carbene and phosphane moieties adopt a *cisoid* coordination, as shown by the C_{NHC}-Ir–P angle of 103°. This coordination mode of the CNP ligand is also manifested in the C_{Py}–N_{Py}–Ir–P and C_{Py}–N_{Py}–Ir–C_{NHC} dihedral angles of 33.63° and –32.28°, respectively, that reflect the substantial flexibility of the CNP ligand.[18] Moreover, there are short H-Cl contacts between the axial methylene CH_2P hydrogens (2.61 Å) and the chloro ligands (sum of the van der Waals radii = 2.9–3.0 Å).[33] In solution, the ^1H NMR spectrum of **8** shows the resonances corresponding to the CH_2P bridges as

Full Paper
doi.org/10.1002/ejic.202000681

two mutually coupled doublet of doublets at δ = 4.26 ($^2J_{HH}$ = 16.6 Hz, $^2J_{HP}$ = 10.2 Hz) and 3.99 ($^2J_{HP}$ = 11.2 Hz), while the hydrogens of the Py–CHN fragments appear as an overlapped signal at 6.59 ppm. Nevertheless, a meaningful $^{13}C\{^1H\}$ NMR spectrum of **8** could not be registered due to its low solubility.

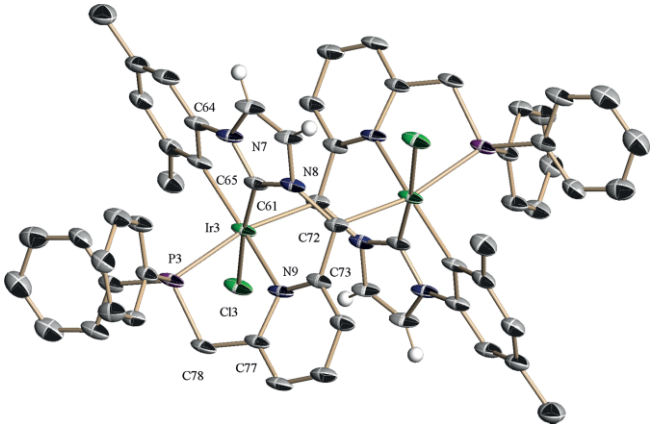

Figure 5. ORTEP drawing at 30 % ellipsoid probability of complex **8**. Hydrogen atoms, except NHC hydrogens, have been omitted for clarity. Selected bond lengths [Å] and angles [°]: Ir(1)–C(1) 1.922(7), Ir(1)–N(3) 2.195(5), Ir(1)–P(1) 2.3034(17), Ir(1)–Cl(1) 2.4901(15), Ir(1)–C(5) 2.074(7), Ir(1)–C(42) 2.156(6), C(1)–Ir(1)–P(1) 103.11(18), C(1)–Ir(1)–C(5) 79.5(3), C(1)–Ir(1)–N(3) 83.9(2), P(1)–Ir(1)–N(3) 77.20(15).

In an attempt to prevent the observed process leading to **7**, reaction of **1** with KO*t*Bu was carried out in the presence of PPh_3, yielding the P-bridge deprotonated complex **9** (Scheme 4). The ^1H NMR spectrum of **9** shows a doublet of doublet at –12.55 ppm with a large $^2J_{HP}$ coupling constant of 138.4 Hz and a small $^2J_{HP}$ of 22.0 Hz, indicative of the presence of phosphane donors *trans* and *cis* to the hydrido ligand, respectively. Moreover, two doublet signals are observed for the methylene protons of the CH_2N bridge appearing at 4.32 and 4.05 ppm ($^2J_{HH}$ = 14.8 Hz), while the phosphane arm produces a singlet at 4.02 ppm, integrating to 1 H,[18] Also, the resonances of the pyridine protons show significant upfield shifts as a consequence of the ligand dearomatization, appearing between 5.43 and 6.48 ppm. The $^{31}P\{^1H\}$ NMR spectrum revealed two mutually coupled doublet signals at δ = –15.3 and 1.1 (J_{PP} = 23 Hz), corresponding to PPh_3 and the phosphorus atom of the lutidine-derived ligand, respectively. Finally, diagnostic resonances in the $^{13}C\{^1H\}$ NMR spectrum of **9** include a doublet at 77.4 ppm (J_{CP} = 70 Hz), assignable to the CHP carbon, and a doublet of doublets at 173.9 ppm (J_{CP} = 96 Hz, J_{CP} = 6 Hz) produced by the C^2(NHC) carbon.

Confirmation of the structure of **9** was obtained from an X-ray diffraction study of suitable crystals of the complex (Figure 6, Table 3). A shortened C_{Py}–CHP [C(18)–C(17) = 1.363(6) Å] bond length is observed with respect to the C_{Py}–CH_2P [C(18)–C(17) = 1.50 Å] distance in complex **1**. This change is accompanied by a modification of the C-C bond lengths in the pyridine ring, with alternating elongated (C-C = 1.41–1.44 Å) and shortened (C-C = 1.34–1.38 Å) distances (average C-C bond in the pyridine ring of complex **1** = 1.38 Å).

Table 3. Selected bond lengths [Å] and angles [°] for complexes **9** and **10**.

	Complex **9**	Complex **10**
Ir(1)–C(1)	1.967(4)	1.968(6)
Ir(1)–N(3)	2.188(3)	2.186(4)
Ir(1)–P(1)	2.3425(10)	2.3471(16)
Ir(1)–C(5)	2.111(4)	2.099(6)
Ir(1)–H(1)Ir	1.635(18)	1.5095
Ir(1)–P(2)	2.3872(10)	2.3766(15)
C(1)–Ir(1)–P(1)	160.48(11)	159.68(16)
C(1)–Ir(1)–C(5)	77.75(15)	78.2(2)
C(1)–Ir(1)–N(3)	86.27(14)	86.8(2)
P(1)–Ir(1)–N(3)	82.32(9)	82.62(13)
P(1)–Ir(1)–H(1)Ir	79.4(14)	70.4
C(1)–Ir(1)–H(1)Ir	83.1(14)	90.7
P(2)–Ir(1)–H(1)Ir	174.8(14)	173.1

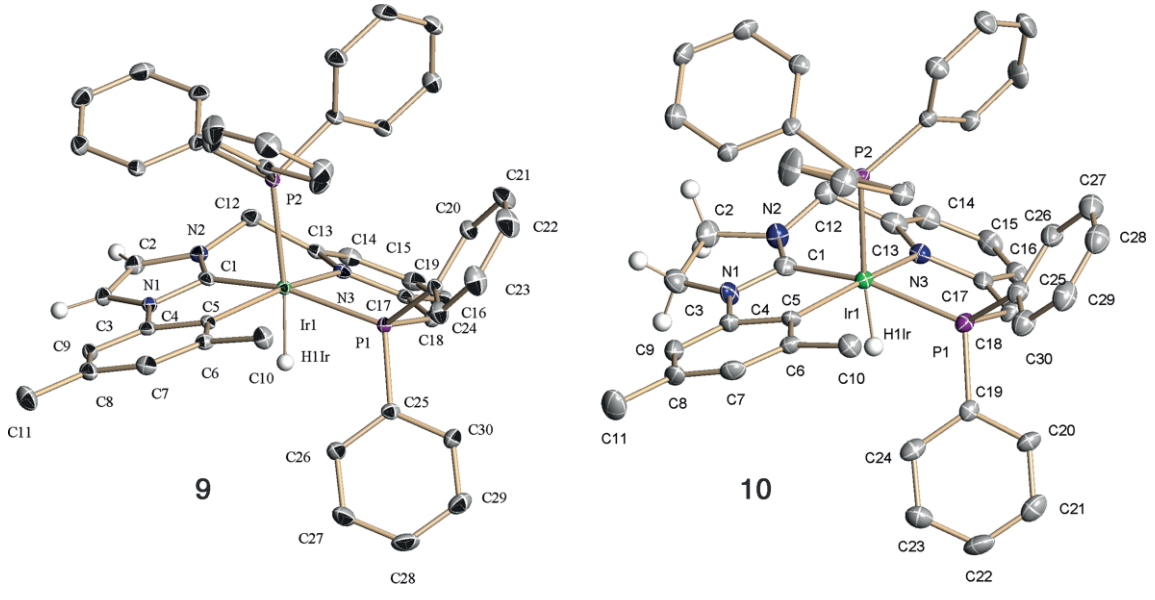

Figure 6. ORTEP drawing at 30 % ellipsoid probability of complexes **9** (left) and **10** (right). Hydrogen atoms, except hydrido ligand and NHC hydrogens, have been omitted for clarity.

Full Paper
doi.org/10.1002/ejic.202000681

Interestingly, complete H/D scrambling of the CHP and CH_2N hydrogens occurs upon addition of CD_3OD to a sample of **9**, suggesting that reversible protonation/deprotonation of both ligand bridges takes place.

Next, the reactivity of complex **6** towards bases was also assessed. While **6** reacted with KO*t*Bu leading to a complex reaction mixture, in the presence of PPh_3 selective deprotonation of the CH_2P arm took place (Scheme 5). The resulting complex **10** shows in their NMR spectra very similar features to those of **9**, including the presence in the ^1H NMR experiment of a doublet of doublets at δ = –12.29 ($^2J_{HP}$ = 132.3, $^2J_{HP}$ = 22.9 Hz) due to the hydrido ligand. The methylene protons of the CH_2N bridge appear in the same experiment as two mutually coupled doublets appearing at 4.72 and 3.78 ppm ($^2J_{HH}$ = 14.1 Hz), while the CHP arm produces a singlet at 3.98 ppm.[18] Also, the upfield shift of the pyridine proton resonances (δ = 5.53–6.49) indicates ligand dearomatization. In the $^{31}P\{^1H\}$ NMR spectrum, two doublet signals are observed at δ = –17.4 and –2.0 ppm (J_{PP} = 25 Hz), corresponding to PPh_3 and the CNP ligand, respectively. Like in the case of complex **9**, the structure of **10** in the solid state demonstrates the dearomatization of the nitrogen-containing central ring of the CNP ligand, as shown by the shortened distance of the C_{Py}–CHP bond [C(18)–C(17) = 1.367(8) Å] in comparison to the C_{Py}–CH_2P [C(18)–C(17) = 1.50 Å] length in complex **6**, as well as the alternating shortened (1.33–1.36 Å) and elongated (1.40–1.45 Å) C-C bonds in the pyridine moiety (Figure 6, Table 3).

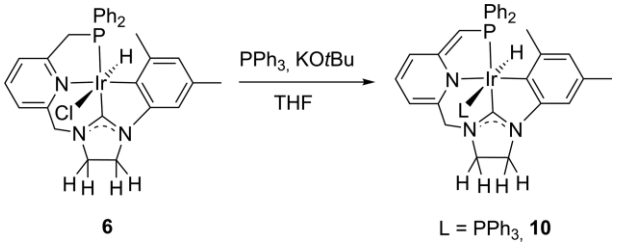

6 L = PPh_3, **10**

Scheme 5. Deprotonation of complex **6** in the presence of PPh_3.

To get further insight into the preferred deprotonation of the various methylene bridges, DFT calculations [B3LYP-D3, 6-31 g(d,p)/SDD] were performed to determine the relative stability of species **I**–**IV**, with **I** and **III** corresponding to the calculated species resulting from removing the PPh_3 ligands from **9** and **10** respectively, and **II** and **IV** to the analogous species resulting from deprotonation of the CH_2–NHC bridge (Figure 7, Table 4; see Supporting Information). In agreement with the formation of species **7**, the calculated species **II** is more stable than its P-arm deprotonated counterpart **I** by ca. 3.2 kcal mol^{-1}. Conversely, species **I·L** (where L = PPh_3, CO, MeCN) resulting from deprotonation of the CH_2P arm are more stable than **II·L**, which is consistent with the formation of **9** and **10**. Thus, analogous trends are observed for imidazolidin-2-ylidene (*s*NHC) containing species **III·L** and **IV·L**. A plausible explanation for the greater stability of **II** and **IV** comes from inspection of their computed structures, which evidences a significant planarity of the dearomatized pyridine ring, the NCN unit of the NHC fragments and the metalated aryl moieties that could facilitate electronic delocalization. Conversely, deprotonation of the CH_2P arm yields vinyl phosphane fragments that destabilize species **I**. These notions are reflected in P–Ir distances that are up to 0.04 Å longer for **I** and **III** than for **II** and **IV**, respectively, and in the relatively shorter N-Ir and NHC-Ir distances found for **II** and **IV** compared to those of **I** and **III**, as well as in the Wiberg bond orders of the metal linkage (Tables S9 and S11). However, in the presence of an additional ligand **L**, derivatives **I·L** and **III·L** are favored, although these exhibit the same trends in their P–Ir, N-Ir and NHC-Ir distances. This rather puzzling result was addressed via Energy Decomposition Analysis (EDA) of the interaction between the L-type ligands and the CNP–Ir(H) moieties in adducts **I·L**–**IV·L**. In this type of analysis, the bonding energy (ΔE_f) is calculated as the energy difference between the adduct and their separate fragments at infinite distance (allowing their geometries to relax), and the interaction energy (ΔE_{int} usually negative) as the energy difference between the adduct and their fragments retaining the geometries they adopt in the complex. The difference is the deformation energy (positive) required for the two fragments to adopt the geometry in their

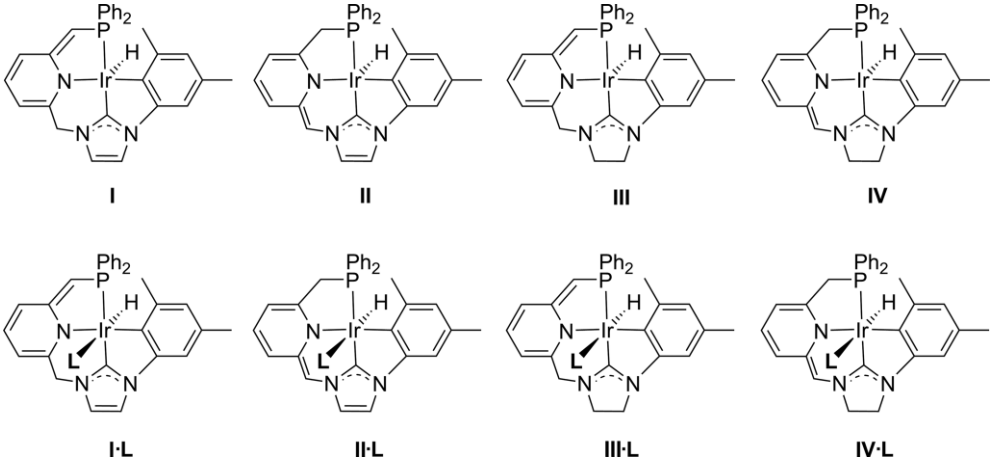

Figure 7. Structures of calculated species **I**–**IV** and **I·L**–**IV·L**.

complexes from their geometry at infinite distance (from $\Delta E_f = \Delta E_{int} + \Delta E_{def}$) (see Supporting Information). Thus EDA of complexes **I·L**–**IV·L** (L = PPh_3, CO) reveals that interaction energies between **L** (L = PPh_3, CO) and metal fragments **I** and **III** are ca. 10 kcal mol^{-1} higher than between the same ligands and **II** and **IV**, which compensates for the greater stability of the latter two. While we cannot offer a clear explanation for this result at this stage, EDA also shows that deformations energies are 2–4 kcal mol^{-1} lower for fragments **I** and **III**, hinting at a higher flexibility of the six-membered Py–Ir–NHC chelate in comparison to the smaller ring involving a CH_2P arm. Both results combine to yield bonding energies 10–13 kcal mol^{-1} higher for the adducts **II·L** and **IV·L** in agreement with the experimental observations.

Table 4. Relative stabilities (ΔE in THF) of **I**–**IV** and **I·L**–**IV·L**.[a]

L	E(**II**)–E(**I**) [kcal mol^{-1}]	E(**IV**)–E(**III**) [kcal mol^{-1}]
–	–3.20	–2.73
PPh_3	7.15	5.46
CO	6.66	5.55
MeCN	2.04	3.16

[a] Energies are relative to the most stable conformer of **I·L**/**II·L** and **III·L**/**IV·L** in each case (see Supporting Information).

Transfer Hydrogenation of Ketones

In comparison to the low stability of the dihydride complex **2** towards the release of H_2, the imidazolidin-2-ylidene derivative **3** is stable in the solid state under ambient conditions. This makes **3** a potentially useful catalytic precursor. In order to initially assess the catalytic potential of complex **3**, its performance in the transfer hydrogenation of ketones using 2-propanol as hydrogen source was studied (Table 5).[34] Using 1.0 mol-% of **3**, under base-free conditions, the reduction of 4-methylacetophenone was performed at 80 °C with 97 % conversion (entry 1). Similarly, high conversions were obtained in the case of acetophenone derivatives bearing *p*-chloro, *o*-bromo, *p*-nitro and *p*-trifluoromethyl substituents (entries 2–5). Finally, the hydrogenation of cyclic ketones, such as α-tetralone and cyclohexanone, also provided high yields of the corresponding alcohols (entries 6 and 7).

Table 5. Transfer hydrogenation of ketones catalyzed by complex **3**.[a]

Entry	Ketone	Conv. [%]
1	4-Methylacetophenone	97
2	4-Chloroacetophenone	94
3	2-Bromoacetophenone	99
4	4-Nitroacetophenone	> 99
5	4-(Trifluoromethyl)acetophenone	> 99
6	α-Tetralone	89
7	Cyclohexanone	> 99

[a] Reaction conditions: 1.0 mol-% complex **3**, 2-propanol, 80 °C, 24 h. [S] = 0.15 M. Conversions were determined by ^{1}H NMR spectroscopy.

Conclusions

As previously reported, the iridium complex **1** featuring a metalated lutidine-derived CNP ligand containing an imidazolin-2-ylidene fragment react with H_2 in the presence of base (KO*t*Bu) initially yielding the dihydride complex **2** in a ligand-assisted H-H activation. Upon prolonged exposure to H_2, complex **2** is hydrogenated at the imidazolin-2-ylidene –CH=CH– moiety leading to the imidazolidin-2-ylidene dihydride derivative **3**. In contrast to complex **2**, which easily losses H_2 leading to the formation of the bimetallic species **7**, the dihydride **3** is stable in solution and in the solid state. This difference is expected to arise from the presence of a better electron-donating imidazolidin-2-ylidene fragment in **3**. Furthermore, the catalytic competence of complex **3** in the base-free transfer hydrogenation of a series of ketones using 2-propanol as hydrogen source has been demonstrated.

Comparison of the structures of the chlorohydride derivatives **6** and **1** shows that both complexes are isostructural, with minor differences arising from the NHC rings. Also the photophysical properties of complexes **1** and **6** are very similar, both showing luminescence from a triplet excited state of mixed MLCT/ILCT character involving the cyclometalated ligand, with the exception that **1** emits strongly at 298 K in the solid state, while its imidazolidin-2-ylidene counterpart is a very weak emitter. The reactivity of complexes **1** and **6** towards bases allows us to compare the relative acidities of the methylene CH_2–P, CH_2–*u*NHC and CH_2–*s*NHC bridges. Deprotonation of **1** and **6** with KO*t*Bu in the presence of PPh_3 leads to the selective deprotonation of the P-bonded methylene bridge; meanwhile, the reaction of **1** in the absence of PPh_3 produces the formation of the bimetallic complex **7**, likely arising from the deprotonation of the CH_2–*u*NHC arm and subsequent dimerization of the resulting halogen-free species. DFT calculations show a slightly higher stability of the NHC-arm deprotonated tautomers **II** and **IV**. However, a reverse stability order is observed for hexacoordinated tautomers **I·L** and **III·L** (L = PPh_3, CO, MeCN), what might be partially attributed to the higher flexibility of the CH_2–NHC containing chelates that should facilitate the accommodation of an additional L ligand.

Overall, the results collected herein demonstrate that, as previously shown with *u*NHCs,[11–17] imidazolidin-2-ylidenes can also be employed as side donors in the design of lutidine-derived complexes capable to participate in ligand-assisted processes. This fact significantly broadens the structural and electronic diversity of this class of proton-responsive ligands.

Experimental Section

General Procedures

All reactions and manipulations were performed under nitrogen or argon, either in a Braun Labmaster 100 glovebox or using standard Schlenk-type techniques. All solvents were distilled under nitrogen with the following desiccants: sodium/benzophenone-ketyl for diethyl ether (Et_2O) and tetrahydrofuran (THF); sodium for pentane and toluene; CaH_2 for dichloromethane and acetonitrile (CH_2Cl_2, CH_3CN). Imidazolium salt **4** was prepared as described previously.[18] Synthesis and characterization of complexes **1**, **3** and **7** have been previously communicated.[21] All other reagents were purchased from commercial suppliers and used as received. NMR spectra were obtained on Bruker DPX-300, DRX-400, AVANCEIII/ASCEND 400R or DRX-500 spectrometers. $^{31}P\{^1H\}$ NMR shifts were

referenced to external 85 % H_3PO_4, while $^{13}C\{^1H\}$ and ^1H shifts were referenced to the residual signals of deuterated solvents. All data are reported in ppm downfield from Me_4Si. All NMR measurements were carried out at 25 °C, unless otherwise stated. NMR signal assignations were confirmed by 2D NMR spectroscopy (^1H-^1H COSY, ^1H-^1H NOESY, ^1H-^{13}C HSQC and ^1H-^{13}C HMBC) for all the complexes. Due to the low solubility of complexes **6**–**10**, NMR spectra were registered using impure samples that were prepared before complete purification and drying of the compounds. Elemental analyses were run by the Analytical Service of the Instituto de Investigaciones Químicas in a Leco TrueSpec CHN elemental analyzer. IR spectra were acquired on a Bruker Tensor 27 instrument.

Deposition Numbers 1581044 (for **6**), 1944657 (for **8**), 1944658 (for **9**), and 1944659 (for **10**) contain the supplementary crystallographic data for this paper. These data are provided free of charge by the joint Cambridge Crystallographic Data Centre and Fach informationszentrum Karlsruhe Access Structures service www.ccdc.cam.ac.uk/structures.

Photophysical Studies

UV/Vis absorption spectra were recorded on a Perkin-Elmer Lambda 750S spectrophotometer. Excitation and emission spectra were recorded on a Jobin Yvon Fluorolog 3–22 spectrofluorometer with a 450 W xenon lamp, double-grating monochromators, and a TBX-04 photomultiplier. The solid-state measurements were made in a front-face configuration using polycrystalline samples between quartz coverslips; the solution measurements were carried out in a right angle configuration using degassed solutions of the samples in 5 mm quartz NMR tubes. A liquid nitrogen Dewar with quartz windows was employed for the low-temperature measurements. Emission lifetimes (τ) were measured using either the Fluorolog's FL-1040 phosphorimeter accessory ($\tau > 10$ μs) or an IBH FluoroHub TCSPC controller and a NanoLED pulse diode excitation source ($\tau < 10$ μs); the estimated uncertainty is ±10 % or better. Emission quantum yields (Φ) were measured using a Hamamatsu C11347 Absolute PL Quantum Yield Spectrometer; the estimated uncertainty is ±5 % or better.

Computational Details

DFT calculations were carried out with the Gaussian 09 program.[35] The hybrid functional B3LYP[36] was used, with dispersion effects taken into account by adding the D3 version of Grimme's empirical dispersion.[37] C, H, N, O and P atoms were represented by the 6-31g(d,p) basis set,[38] whereas Ir was described using the Stuttgart/Dresden Effective Core Potential and its associated basis set SDD.[39] All geometry optimizations were performed without restrictions in THF (bulk solvent effects modelled with the SMD continuum model).[40] The EDA analysis has been performed using the counterpoise correction as implemented in Gaussian09.[41] Wiberg bond orders in the Lowdin orthogonalized basis[42] have been calculated with the Multiwn software.[43]

Synthesis of Metalated Ir–CNP Complexes

Complex 1:[21] A solution of imidazolium salt **4** (0.083 g, 0.167 mmol) in CH_2Cl_2 (5 mL) was treated with Ag_2O (0.020 g, 0.085 mmol), and the mixture was stirred at the dark for 20 h. The suspension was filtered and added to a solution of $[IrCl(COE)_2]_2$ (0.074 g, 0.083 mmol) in CH_2Cl_2 (10 mL). The resulting solution was stirred overnight and filtered. Solvent was removed under reduced pressure, and the residue was washed with Et_2O (3 × 5 mL) and dried under vacuum. Yellow solid (0.104 g, 91 %).

Complex 6: A solution of complex **3** (0.100 g, 0.15 mmol) in CH_2Cl_2 (7 mL) was stirred for 6 h. Solvent was evaporated, and the resulting solid was washed with Et_2O (3 × 5 mL) and pentane (3 × 5 mL) and dried under vacuum. Pale yellow solid (0.090 g, 86 %). Crystals suitable for X-ray diffraction analysis were grown from a saturated solution of complex **6** in THF. ^1H NMR (400 MHz, CD_2Cl_2): δ = 7.85 (dd, $^3J_{HH}$ = 8.9 Hz, $^3J_{HP}$ = 6.8 Hz, 2H, 2 H arom PPh), 7.72 (m, 3H, 2 H arom PPh + H arom Py), 7.53 (d, $^3J_{HH}$ = 8.0 Hz, 1H, H arom Py), 7.40 (m, 6H, 6 H arom PPh), 7.23 (d, $^3J_{HH}$ = 8.0 Hz, 1H, H arom Py), 6.47 (s, 1H, H arom Xyl), 6.35 (s, 1H, H arom Xyl), 5.32 (d, $^2J_{HH}$ = 16.0 Hz, 1H, NC*H*H), 4.67 (d, $^2J_{HH}$ = 16.0 Hz, 1H, NC*H*H), 4.42 (dd, $^2J_{HH}$ = 16.0 Hz, $^2J_{HP}$ = 8.0 Hz, 1H, PC*H*H), 4.13 (m, 4H, 4 C*H*H NHC), 3.87 (dd, $^2J_{HH}$ = 16.0 Hz, $^2J_{HP}$ = 8.0 Hz, 1H, PC*H*H), 2.31 (s, 3H, CH_3), 2.01 (s, 3H, CH_3), –22.26 (d, $^2J_{HP}$ = 16.0 Hz, 1H, IrH); $^{31}P\{^1H\}$ NMR (121 MHz, CD_2Cl_2): δ = 11.5; $^{13}C\{^1H\}$ NMR (101 MHz, CD_2Cl_2): δ = 203.9 (d, J_{CP} = 113 Hz, C-2 NHC), 165.3 (d, J_{CP} = 5 Hz, C_q arom), 156.4 (C_q arom), 151.1 (d, J_{CP} = 4 Hz, C_q arom), 145.4 (C_q arom), 137.0 (CH arom), 134.7 (d, J_{CP} = 48 Hz, C_q arom), 134.7 (d, J_{CP} = 12 Hz, 2 CH arom), 133.5 (d, J_{CP} = 9 Hz, 2 CH arom), 131.8 (C_q arom), 131.0 (d, J_{CP} = 2 Hz, CH arom), 129.9 (d, J_{CP} = 2 Hz, CH arom), 128.8 (d, J_{CP} = 10 Hz, 2 CH arom), 128.3 (d, J_{CP} = 9 Hz, 2 CH arom), 123.8 (CH arom), 122.7 (CH arom), 122.1 (d, J_{CP} = 8 Hz, CH arom), 107.8 (CH arom), 57.5 (CH_2N), 52.6 (d, J_{CP} = 5 Hz, CH_2 NHC), 48.8 (d, J_{CP} = 29 Hz, CH_2P), 47.0 (d, J_{CP} = 4 Hz, CH_2 NHC), 29.3 (d, J_{CP} = 6 Hz, CH_3), 20.8 (CH_3), signals for two C_q could not be detected due to the low solubility of the complex; IR (nujol): $\tilde{\nu}$ = 2151 (ν_{IrH}) cm^{-1}; Anal. Calcd (%) for $C_{30}H_{30}IrClN_3P$: C 52.13, H 4.37, N 6.08; found C 52.14, H 4.45, N 6.08.

Complex 8: A suspension of complex **7** (0.052 g, 0.04 mmol) in $CHCl_3$ (7 mL) was stirred for 3 h at 50 °C. Solvent was evaporated, and the resulting solid was washed with Et_2O (3 × 5 mL) and pentane (3 × 5 mL), and dried under vacuum. Pale yellow solid (0.040 g, 84 %). Crystals suitable for X-ray diffraction analysis were grown from a saturated solution of complex **8** in THF. $^{13}C\{^1H\}$ NMR spectrum of **8** could not be registered due to the low solubility of the complex in common deuterated solvents. ^1H NMR (300 MHz, CD_2Cl_2): δ = 8.09 (m, 4H, 4 H arom PPh), 7.70 (m, 8H, 8 H arom), 7.33 (m, 4H, 4 H arom), 7.24 (m, 6H, 6 H arom PPh), 7.06 (d, $^3J_{HH}$ = 7.4 Hz, 2H, 2 H arom Py), 6.85 (m, 4H, 2 H arom Py + 2 H arom NHC), 6.59 (m, 6H, 4 H arom + 2 NCH-Py), 6.05 (d, $^3J_{HH}$ = 7. 8 Hz, 2H, 2 H arom Py), 4.26 (dd, $^2J_{HH}$ = 16.6 Hz, $^2J_{HP}$ = 10.2 Hz, 2H, 2 PC*H*H), 3.99 (dd, $^2J_{HH}$ = 16.7 Hz, $^2J_{HP}$ = 11.2 Hz, 2H, 2 PC*H*H), 3.04 (s, 6H, 2 CH_3), 2.43 (s, 6H, 2 CH_3); $^{31}P\{^1H\}$ NMR (121 MHz, CD_2Cl_2): δ = –0.9; Anal. Calcd (%) for $C_{60}H_{52}Cl_2Ir_2N_6P_2$: C 52.43, H 3.81, N 6.11; found C 52.50, H 3.70, N 6.08.

Complex 9: A suspension of **1** (0.047 g, 0.068 mmol) and PPh_3 (0.018 g, 0.068 mmol) in THF (2 mL) was treated with KO*t*Bu (0.008 g, 0.069 mmol). The reaction mixture was stirred for 2 h and filtered. The solvent was removed under vacuum and the resulting solid was washed with Et_2O (3 × 3 mL) and pentane (3 × 3 mL) to yield complex **9** as a pale brown solid (0.048 g, 77 %).

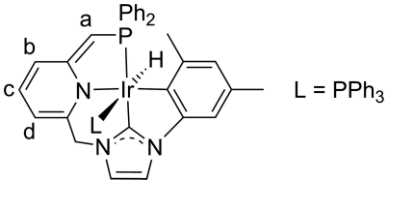

^1H NMR (400 MHz, [D$_8$]THF, 323 K): δ = 7.61 (d, J_{HH} = 1.6 Hz, 1H, H arom NHC), 7.57 (m, 2H, 2 H arom Ph), 7.43 (dd, J_{HP} = 8.8 Hz, $^3J_{HH}$ = 7.3 Hz, 2H, 2 H arom Ph), 7.18 (m, 4H, 4 H arom Ph), 7.07 (m, 3H, 3 H arom), 7.03 (d, J_{HH} = 1.6 Hz, 1H, H arom NHC), 6.95 (m, 8H, 8 H arom), 6.87 (m, 1H, H arom), 6.67 (dd, J_{HP} = 8.8 Hz, $^3J_{HH}$ = 8.8 Hz, 6

H arom Ph), 6.48 (m, 3H, H arom + H^c + H^b), 5.43 (d, $^3J_{HH}$ = 6.1 Hz, 1H, H^d), 4.32 (d, $^2J_{HH}$ = 14.8 Hz, 1H, NC*H*H), 4.05 (d, $^2J_{HH}$ = 14.8 Hz, 1H, NC*H*H), 4.02 (s, 1H, H^a), 2.35 (s, 3H, CH_3), 1.61 (s, 3H, CH_3), –12.55 (dd, $^2J_{HP}$ = 138.4 Hz, $^2J_{HP}$ = 22.0 Hz, 1H, IrH); $^{31}P\{^1H\}$ NMR (162 MHz, [D$_8$]THF): δ = 1.1 (d, J_{PP} = 23 Hz, CH_2PPh_2), –15.3 (d, J_{PP} = 23 Hz, PPh_3); $^{13}C\{^1H\}$ NMR (101 MHz, [D$_8$]THF, 323 K): δ = 173.9 (dd, J_{CP} = 96 Hz, J_{CP} = 6 Hz, C-2 NHC), 173.8 (d, J_{CP} = 18 Hz, C_q arom), 150.6 (C_q arom), 148.9 (2 C_q arom), 145.8 (dd, J_{CP} = 39 Hz, J_{CP} = 3 Hz, C_q arom), 144.0 (dd, J_{CP} = 58 Hz, J_{CP} = 4 Hz, C_q arom), 137.7 (d, J_{CP} = 36 Hz, 3 C_q arom), 135.4 (d, J_{CP} = 11 Hz, 2 CH arom), 134.5 (d, J_{CP} = 10 Hz, 2 CH arom), 134.1 (d, J_{CP} = 11 Hz, 6 CH arom), 131.5 (C_q arom), 130.6 (d, J_{CP} = 3 Hz, CH Py), 129.1 (3 CH arom), 128.3 (CH arom), 128.0 (m, 6 CH arom), 127.9 (CH arom), 127.5 (d, J_{CP} = 4 Hz, 2 CH arom), 127.4 (d, J_{CP} = 5 Hz, 2 CH arom), 125.7 (CH arom), 124.3 (br, Ir-C_q arom), 118.8 (d, J_{CP} = 3 Hz, CH arom), 115.4 (d, J_{CP} = 16 Hz, CH Py), 114.4 (d, J_{CP} = 3 Hz, CH arom), 109.7 (CH arom), 102.4 (C^d), 77.4 (d, J_{CP} = 70 Hz, C^a), 56.7 (CH_2N), 29.7 (d, J_{CP} = 5 Hz, CH_3), 20.8 (CH_3); IR (nujol): $\tilde{\nu}$ = 2053 (ν_{IrH}) cm^{-1}; Anal. Calcd (%) for $C_{48}H_{42}IrN_3P_2$: C 63.00, H 4.63, N 4.59; found C 63.49, H 4.96, N 4.63.

Complex 10: A suspension of **6** (0.054 g, 0.078 mmol) and PPh_3 (0.020 g, 0.078 mmol) in THF (2 mL) was treated with KO*t*Bu (0.009 g, 0.080 mmol). The reaction mixture was stirred for 2 h and filtered. The solvent was removed under vacuum and the resulting solid was washed with Et_2O (3 × 3 mL) and pentane (3 × 3 mL) to yield complex **10** as a yellow solid (0.051 g, 71 %). Suitable crystals for X-ray diffraction analysis were grown from a saturated solution of complex **10** in Et_2O.

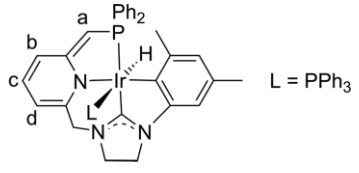

^1H NMR (400 MHz, [D$_8$]THF): δ = 7.57 (m, 2H, 2 H arom PPh), 7.43 (dd, J_{HP} = 8.5 Hz, $^3J_{HH}$ = 7.3 Hz, 2H, 2 H arom PPh), 7.24 (m, 2H, 2 H arom PPh), 7.20 (m, 1H, H arom PPh), 7.06 (m, 8H, 8 H arom PPh), 6.98 (m, 2H, 2 H arom PPh), 6.72 (br m, 8H, 8 H arom PPh), 6.46 (m, 2H, H^b + H^d), 6.36 (s, 1H, H arom), 6.32 (s, 1H, H arom), 5.53 (dd, $^3J_{HH}$ = 3.9 Hz, $^3J_{HH}$ = 3.8 Hz, 1H, H^c), 3.99 (m, 1H, C*H*H NHC), 3.98 (s, 1H, H^a), 3.89 (m, 2H, 2 C*H*H NHC), 3.78 (d, $^2J_{HH}$ = 14.1 Hz, 1H, NC*H*H), 3.55 (d, $^2J_{HH}$ = 14.1 Hz, 1H, NC*H*H), 2.84 (m, 1H, C*H*H NHC), 2.32 (s, 3H, CH_3), 1.46 (s, 3H, CH_3), –12.25 (dd, $^2J_{HP}$ = 132.8 Hz, $^2J_{HP}$ = 23.1 Hz, 1H, IrH); $^{31}P\{^1H\}$ NMR (121 MHz, [D$_8$]THF): δ = –2.0 (d, J_{PP} = 25 Hz, CH_2PPh_2), –17.4 (d, J_{PP} = 25 Hz, PPh_3); $^{13}C\{^1H\}$ NMR (101 MHz, [D$_8$]THF): δ = 173.5 (d, J_{CP} = 18 Hz, C_q arom), 152.0 (C_q arom), 151.5 (C_q arom), 147.4 (C_q arom), 146.1 (d, J_{CP} = 38 Hz, C_q arom), 144.1 (d, J_{CP} = 58 Hz, C_q arom), 35.4 (d, J_{CP} = 11 Hz, 2 CH arom), 134.4 (br m, 10 CH arom), 131.4 (C_q arom), 130.9 (CH Py), 129.4 (2 CH arom), 128.2 (CH arom), 128.0 (br m, 6 CH arom), 127.4 (d, J_{CP} = 7 Hz, 2 CH arom), 127.3 (d, J_{CP} = 8 Hz, 2 CH arom), 122.8 (CH arom), 114.6 (d, J_{CP} = 16 Hz, CH Py), 107.2 (CH arom), 101.9 (C^d), 76.7 (d, J_{CP} = 70 Hz, C^a), 56.6 (CH_2N), 51.3 (CH_2 NHC), 46.6 (CH_2 NHC), 29.1 (d, J_{CP} = 4 Hz, CH_3), 21.0 (CH_3), the C^2(NHC) and 4 C_q carbon signals could not be detected due to significant line broadening and the low solubility of the complex in [D$_8$]THF; IR (nujol): $\tilde{\nu}$ = 2082 (ν_{IrH}) cm^{-1}; Anal. Calcd (%) for $C_{48}H_{44}IrN_3P_2$: C 62.87, H 4.84, N 4.58; found C 62.72, H 5.06, N 4.42.

Transfer Hydrogenation of Ketones

A solution of complex **3** (1.0 mg, 1.5 μmol) and the corresponding ketone (0.15 mmol) in 2-propanol (1.0 mL) was heated to 80 °C for 24 h. Conversion was determined after solvent evaporation by ^1H NMR spectroscopy using mesitylene as internal standard.

Acknowledgments

Financial support (FEDER contribution) from the Spanish Ministerio de Ciencia, Innovación y Universidades (CTQ2015-69568-P, CTQ2016-75193-P, CTQ2016-80814-R and CTQ2016-81797-REDC), Fundación Séneca (19890/GERM/15), and Junta de Andalucía (PY18-3208) is gratefully acknowledged. M. H. J. thanks SECITI-DF for a postdoctoral fellowship, and CONACyT Mexico for postdoctoral funding (263719). The use of computational facilities of the Supercomputing Centre of Galicia (CESGA) is gratefully acknowledged.

Keywords: Ligand design · Proton-responsive ligands · Carbene ligands · Luminescence · Hydrogenation

[1] a) J. R. Khusnutdinova, D. Milstein, *Angew. Chem. Int. Ed.* **2015**, *54*, 12236–12273; *Angew. Chem.* **2015**, *127*, 12406; b) J. I. van der Vlugt, *Eur. J. Inorg. Chem.* **2012**, 363–375; c) H. Grützmacher, *Angew. Chem. Int. Ed.* **2008**, *47*, 1814–1818; *Angew. Chem.* **2008**, *120*, 1838.

[2] a) J. I. van der Vlugt, J. N. H. Reek, *Angew. Chem. Int. Ed.* **2009**, *48*, 8832–8846; *Angew. Chem.* **2009**, *121*, 8990; b) C. Gunanathan, D. Milstein, *Acc. Chem. Res.* **2011**, *44*, 588–602; c) D. Milstein, *Phil. Trans. R. Soc. A* **2015**, *373*, 20140189; d) T. Zell, D. Milstein, *Acc. Chem. Res.* **2015**, *48*, 1979–1994.

[3] For some selected examples of M-PNP and M–PNN complexes: a) J. Zhang, M. Gandelman, L. J. W. Shimon, H. Rozenberg, D. Milstein, *Organometallics* **2004**, *23*, 4026–4033; b) J. Zhang, G. Leitus, Y. Ben-David, D. Milstein, *J. Am. Chem. Soc.* **2005**, *127*, 10840–10841; c) A. Anaby, M. Feller, Y. Ben-David, G. Leitus, Y. Diskin-Posner, L. J. W. Shimon, D. Milstein, *J. Am. Chem. Soc.* **2016**, *138*, 9941–9950; d) M. Vogt, A. Nerush, M. A. Iron, G. Leitus, Y. Diskin-Posner, L. J. W. Shimon, Y. Ben-David, D. Milstein, *J. Am. Chem. Soc.* **2013**, *135*, 17004–17018; e) A. Mukherjee, A. Nerush, G. Leitus, L. J. W. Shimon, Y. Ben-David, N. A. Espinosa Jalapa, D. Milstein, *J. Am. Chem. Soc.* **2016**, *138*, 4298–4301; f) R. Langer, G. Leitus, Y. Ben-David, D. Milstein, *Angew. Chem. Int. Ed.* **2011**, *50*, 2120–2124; *Angew. Chem.* **2011**, *123*, 2168; g) D. Srimani, A. Mukherjee, A. F. G. Goldberg, G. Leitus, Y. Diskin-Posner, L. J. W. Shimon, Y. Ben-David, D. Milstein, *Angew. Chem. Int. Ed.* **2015**, *54*, 12357–12360; *Angew. Chem.* **2015**, *127*, 12534; h) A. Mukherjee, D. Srimani, S. Chakraborty, Y. Ben-David, D. Milstein, *J. Am. Chem. Soc.* **2015**, *137*, 8888–8891.

[4] a) *N-Heterocyclic Carbenes: Effective Tools for Organometallic Synthesis* (Ed.: S. P. Nolan), Wiley-VCH, Weinheim, **2014**; b) M. N. Hopkinson, C. Richter, M. Schedler, F. Glorius, *Nature* **2014**, *510*, 485–496.

[5] a) G. C. Fortman, S. P. Nolan, *Chem. Soc. Rev.* **2011**, *40*, 5151–5169; b) V. Ritleng, M. Henrion, M. J. Chetcuti, *ACS Catal.* **2016**, *6*, 890–906; c) R. D. J. Froese, C. Lombardi, M. Pompeo, R. P. Rucker, M. G. Organ, *Acc. Chem. Res.* **2017**, *50*, 2244–2253.

[6] G. C. Vougioukalakis, R. H. Grubbs, *Chem. Rev.* **2010**, *110*, 1746–1787.

[7] a) S. Kaufhold, L. Petermann, R. Staehle, S. Rau, *Coord. Chem. Rev.* **2015**, *304–305*, 73–87; b) D. Zhao, L. Candish, D. Paul, F. Glorius, *ACS Catal.* **2016**, *6*, 5978–5988; c) H. M. Lee, T. Jiang, E. D. Stevens, S. P. Nolan, *Organometallics* **2001**, *20*, 1255–1258; d) L. D. Vázquez-Serrano, B. T. Owens, J. M. Buriak, *Chem. Commun.* **2002**, 2518–2519; e) C. Gandolfi, M. Heckenroth, A. Neels, G. Laurenczy, M. Albrecht, *Organometallics* **2009**, *28*, 5112–5121; f) J. W. Sprengers, J. Wassenaar, N. D. Clement, K. J. Cavell, C. J. Elsevier, *Angew. Chem. Int. Ed.* **2005**, *44*, 2026–2029; *Angew. Chem.* **2005**, *117*, 2062; g) H. M. Lee, D. C. Smith, Z. He, E. D. Stevens, C. S. Yi, S. P. Nolan, *Organometallics* **2001**, *20*, 794–797.

[8] D. J. Nelson, S. P. Nolan, *Chem. Soc. Rev.* **2013**, *42*, 6723–6753.

[9] N. S. Antonova, J. J. Carbó, J. M. Poblet, *Organometallics* **2009**, *28*, 4283–4287.

[10] a) C.-F. Fu, C.-C. Lee, Y.-H. Liu, S.-M. Peng, S. Warsink, C. J. Elsevier, J.-T. Chen, S.-T. Liu, *Inorg. Chem.* **2010**, *49*, 3011–3018; b) S. Khumsubdee, Y.

Fan, K. Burgess, *J. Org. Chem.* **2013**, *78*, 9969–9974; c) M. Süßner, H. Plenio, *Chem. Commun.* **2005**, 5417–5419; d) S. Leuthäußer, V. Schmidts, C. M. Thiele, H. Plenio, *Chem. Eur. J.* **2008**, *14*, 5465–5481; e) G. De Bo, G. Berthon-Gelloz, B. Tinant, I. E. Markó, *Organometallics* **2006**, *25*, 1881–1890; f) M. Scholl, S. Ding, C. W. Lee, R. H. Grubbs, *Org. Lett.* **1999**, *1*, 953–956; g) A. C. Hillier, W. J. Sommer, B. S. Yong, J. L. Petersen, L. Cavallo, S. P. Nolan, *Organometallics* **2003**, *22*, 4322–4326; h) U. L. Dharmasena, H. M. Foucault, E. N. dos Santos, D. E. Fogg, S. P. Nolan, *Organometallics* **2005**, *24*, 1056–1058; i) J. A. M. Lummiss, C. S. Higman, D. L. Fyson, R. McDonald, D. E. Fogg, *Chem. Sci.* **2015**, *6*, 6739–6746.

[11] a) R. E. Andrew, A. B. Chaplin, *Inorg. Chem.* **2015**, *54*, 312–322; b) R. E. Andrew, L. González-Sebastián, A. B. Chaplin, *Dalton Trans.* **2016**, *45*, 1299–1305; c) R. E. Andrew, A. B. Chaplin, *Dalton Trans.* **2014**, *43*, 1413–1423; d) R. E. Andrew, D. W. Ferdani, C. A. Ohlin, A. B. Chaplin, *Organometallics* **2015**, *34*, 913–917; e) R. E. Andrew, C. M. Storey, A. B. Chaplin, *Dalton Trans.* **2016**, *45*, 8937–8944; f) M. R. Gyton, B. Leforestier, A. B. Chaplin, *Organometallics* **2018**, *37*, 3963–3971; g) C. M. Storey, M. R. Gyton, R. E. Andrew, A. B. Chaplin, *Angew. Chem. Int. Ed.* **2018**, *57*, 12003–12006; *Angew. Chem.* **2018**, *130*, 12179.

[12] G. A. Filonenko, E. Cosimi, L. Lefort, M. P. Conley, C. Copéret, M. Lutz, E. J. M. Hensen, E. A. Pidko, *ACS Catal.* **2014**, *4*, 2667–2671.

[13] G. A. Filonenko, D. Smykowski, B. M. Szyja, G. Li, J. Szczygiel, E. J. M. Hensen, E. A. Pidko, *ACS Catal.* **2015**, *5*, 1145–1154.

[14] Y. Sun, C. Koehler, R. Tan, V. T. Annibale, D. Song, *Chem. Commun.* **2011**, *47*, 8349–8351.

[15] E. Fogler, E. Balaraman, Y. Ben-David, G. Leitus, L. J. W. Shimon, D. Milstein, *Organometallics* **2011**, *30*, 3826–3833.

[16] C. del Pozo, M. Iglesias, F. Sánchez, *Organometallics* **2011**, *30*, 2180–2188.

[17] a) M. Hernández-Juárez, M. Vaquero, E. Álvarez, V. Salazar, A. Suárez, *Dalton Trans.* **2013**, *42*, 351–354; b) M. Hernández-Juárez, J. López-Serrano, P. Lara, J. P. Morales-Cerón, M. Vaquero, E. Álvarez, V. Salazar, A. Suárez, *Chem. Eur. J.* **2015**, *21*, 7540–7555.

[18] P. Sánchez, M. Hernández-Juárez, E. Álvarez, M. Paneque, N. Rendón, A. Suárez, *Dalton Trans.* **2016**, *45*, 16997–17009.

[19] P. Sánchez, M. Hernández-Juárez, N. Rendón, J. López-Serrano, E. Álvarez, M. Paneque, A. Suárez, *Dalton Trans.* **2018**, *47*, 16766–16776.

[20] a) M. Asay, D. Morales-Morales, *Dalton Trans.* **2015**, *44*, 17432–17447; b) B. G. Anderson, J. L. Spencer, *Chem. Eur. J.* **2014**, *20*, 6421–6432; c) A. J. Nawara-Hultzsch, J. D. Hackenberg, B. Punji, C. Supplee, T. J. Emge, B. C. Bailey, R. R. Schrock, M. Brookhart, A. S. Goldman, *ACS Catal.* **2013**, *3*, 2505–2514; d) H. Valdés, M. A. García-Eleno, D. Canseco-Gonzalez, D. Morales-Morales, *ChemCatChem* **2018**, *10*, 3136-3172; e) *Pincer Compounds: Chemistry and Applications* (Ed.: D. Morales-Morales), Elsevier, Netherlands, **2018**.

[21] M. Hernández-Juárez, J. López-Serrano, P. González-Herrero, N. Rendón, E. Álvarez, M. Paneque, A. Suárez, *Chem. Commun.* **2018**, *54*, 3843–3846.

[22] a) J. B. Waters, J. M. Goicoechea, *Coord. Chem. Rev.* **2015**, *293–294*, 80–94; b) T. Simler, P. Braunstein, A. Danopoulos, *Chem. Commun.* **2016**, *52*, 2717–2720; c) A. El-Hellani, V. Lavallo, *Angew. Chem. Int. Ed.* **2014**, *53*, 4489–4493; *Angew. Chem.* **2014**, *126*, 4578; d) W. A. Herrmann, P. W. Roesky, M. Elison, G. Artus, K. Öfele, *Organometallics* **1995**, *14*, 1085–1086; e) A. A. Danopoulos, D. Pugh, J. A. Wright, *Angew. Chem. Int. Ed.* **2008**, *47*, 9765–9767; *Angew. Chem.* **2008**, *120*, 9911.

[23] M. Albrecht, *Chem. Rev.* **2010**, *110*, 576–623.

[24] D. Tapu, D. A. Dixon, C. Roe, *Chem. Rev.* **2009**, *109*, 3385–3407.

[25] M. S. Viciu, O. Navarro, R. F. Germaneau, R. A. Kelly III, W. Sommer, N. Marion, E. D. Stevens, L. Cavallo, S. P. Nolan, *Organometallics* **2004**, *23*, 1629–1635.

[26] J. C. Deaton, F. N. Castellano in *Iridium(III) in Optoelectronic and Photonics Applications* (Ed.: E. Zysman-Colman), John Wiley & Sons, Chichester, **2017**, pp 1–69.

[27] For some examples of luminescence studies of NHC-Ir complexes: a) T. Sajoto, P. I. Djurovich, A. Tamayo, M. Yousufuddin, R. Bau, M. E. Thompson, R. J. Holmes, S. R. Forrest, *Inorg. Chem.* **2005**, *44*, 7992–8003; b) J. Lee, H.-F. Chen, T. Batagoda, C. Coburn, P. I. Djurovich, M. E. Thompson, S. R. Forrest, *Nat. Mater.* **2016**, *15*, 92–98; c) F. Kessler, R. D. Costa, D. Di Censo, R. Scopelliti, E. Ortí, H. J. Bolink, S. Meier, W. Sarfert, M. Grätzel, M. K. Nazeeruddin, E. Baranoff, *Dalton Trans.* **2012**, *41*, 180–191; d) J. Torres, M. C. Carrión, J. Leal, F. A. Jalón, J. V. Cuevas, A. M. Rodríguez, G. Castañeda, B. R. Manzano, *Inorg. Chem.* **2018**, *57*, 970–984; e) C. Yang, F. Mehmood, T. L. Lam, S. L. F. Chan, Y. Wu, C. S. Yeung, X. Guan, K. Li, C. Y. S. Chung, C. Y. Zhou, X. Guan, C.-M. Che, *Chem. Sci.* **2016**, *7*, 3123–3136; f) C. H. Yang, J. Beltran, V. Lemaur, J. Cornil, D. Hartmann, W. Sarfert, R. Fröhlich, C. Bizzarri, L. De Cola, *Inorg. Chem.* **2010**, *49*, 9891–9901.

[28] P. Chen, T. J. Meyer, *Chem. Rev.* **1998**, *98*, 1439–1478.

[29] H. Yersin, A. F. Rausch, R. Czerwieniec, T. Hofbeck, T. Fischer, *Coord. Chem. Rev.* **2011**, *255*, 2622–2652.

[30] a) C. Hou, J. Jiang, Y. Li, C. Zhao, Z. Ke, *ACS Catal.* **2017**, *7*, 786–795; b) X. Yang, M. B. Hall, *J. Am. Chem. Soc.* **2010**, *132*, 120–130.

[31] For some examples of reactions of deprotonated lutidine-derived complexes with electrophiles, see: a) J. I. van der Vlugt, E. A. Pidko, D. Vogt, M. Lutz, A. L. Spek, *Inorg. Chem.* **2009**, *48*, 7513–7515; b) C. A. Huff, J. W. Kampf, M. S. Sanford, *Organometallics* **2012**, *31*, 4643–4645; c) C. A. Huff, J. W. Kampf, M. S. Sanford, *Chem. Commun.* **2013**, *49*, 7147–7149; d) S. Perdriau, D. S. Zijlstra, H. J. Heeres, J. G. de Vries, E. Otten, *Angew. Chem. Int. Ed.* **2015**, *54*, 4236–4240; *Angew. Chem.* **2015**, *127*, 4310; e) M. Vogt, A. Nerush, Y. Diskin-Posner, Y. Ben-David, D. Milstein, *Chem. Sci.* **2014**, *5*, 2043–2051; f) M. Montag, J. Zhang, D. Milstein, *J. Am. Chem. Soc.* **2012**, *134*, 10325–10328.

[32] M. Gargir, Y. Ben-David, G. Leitus, Y. Diskin-Posner, L. J. W. Shimon, D. Milstein, *Organometallics* **2012**, *31*, 6207–6214.

[33] a) R. S. Rowland, R. Taylor, *J. Phys. Chem.* **1996**, *100*, 7384–7391; b) J. Reedijk, *Chem. Soc. Rev.* **2013**, *42*, 1776–1783.

[34] D. Wang, D. Astruc, *Chem. Rev.* **2015**, *115*, 6621–6686.

[35] M. J. Frisch, G. W. Trucks, H. B. Schlegel, G. E. Scuseria, M. A. Robb, J. R. Cheeseman, G. Scalmani, V. Barone, B. Mennucci, G. A. Petersson, H. Nakatsuji, M. Caricato, X. Li, H. P. Hratchian, A. F. Izmaylov, J. Bloino, G. Zheng, J. L. Sonnenberg, M. Hada, M. Ehara, K. Toyota, R. Fukuda, J. Hasegawa, M. Ishida, T. Nakajima, Y. Honda, O. Kitao, H. Nakai, T. Vreven, J. A. Montgomery Jr., J. E. Peralta, F. Ogliaro, M. Bearpark, J. J. Heyd, E. Brothers, K. N. Kudin, V. N. Staroverov, R. Kobayashi, J. Normand, K. Raghavachari, A. Rendell, J. C. Burant, S. S. Iyengar, J. Tomasi, M. Cossi, N. Rega, J. M. Millam, M. Klene, J. E. Knox, J. B. Cross, V. Bakken, C. Adamo, J. Jaramillo, R. Gomperts, R. E. Stratmann, O. Yazyev, A. J. Austin, R. Cammi, C. Pomelli, J. W. Ochterski, R. L. Martin, K. Morokuma, V. G. Zakrzewski, G. A. Voth, P. Salvador, J. J. Dannenberg, S. Dapprich, A. D. Daniels, Ö. Farkas, J. B. Foresman, J. V. Ortiz, J. Cioslowski, D. J. Fox, *Gaussian 09, Revision E.01*, Gaussian, Inc., Wallingford CT, **2016**.

[36] a) A. D. Becke, *J. Chem. Phys.* **1993**, *98*, 5648–5652; b) C. Lee, W. Yang, R. G. Parr, *Phys. Rev. B* **1988**, *37*, 785–789; c) B. Miehlich, A. Savin, H. Stoll, H. Preuss, *Chem. Phys. Lett.* **1989**, *157*, 200–206.

[37] S. Grimme, S. Ehrlich, L. Goerigk, *J. Comput. Chem.* **2011**, *32*, 1456–1465.

[38] a) R. Ditchfield, W. J. Hehre, J. A. Pople, *J. Chem. Phys.* **1971**, *54*, 724–728; b) W. J. Hehre, R. Ditchfield, J. A. Pople, *J. Chem. Phys.* **1972**, *56*, 2257–2261; c) P. C. Hariharan, J. A. Pople, *Theor. Chim. Acta* **1973**, *28*, 213–222; d) M. M. Francl, W. J. Pietro, W. J. Hehre, J. S. Binkley, M. S. Gordon, D. J. DeFrees, J. A. Pople, *J. Chem. Phys.* **1982**, *77*, 3654–3665.

[39] D. Andrae, U. Haeussermann, M. Dolg, H. Stoll, H. Preuss, *Theor. Chim. Acta* **1990**, *77*, 123–141.

[40] A. V. Marenich, C. J. Cramer, D. G. Truhlar, *J. Phys. Chem. B* **2009**, *113*, 6378–6396.

[41] a) S. F. Boys, F. Bernardi, *Mol. Phys.* **1970**, *19*, 553–556; b) S. Simon, M. Duran, J. J. Dannenberg, *J. Chem. Phys.* **1996**, *105*, 11024–11031.

[42] O. V. Sizova, L. V. Skripnikov, A. Yu. Sokolov, *THEOCHEM* **2008**, *870*, 1–9.

[43] T. Lu, F. Chen, *J. Comput. Chem.* **2012**, *33*, 580–592; ; Multiwfn 3.6 (http://sobereva.com/multiwfn/).

Received: July 17, 2020

Lutidine-Derived Ligands

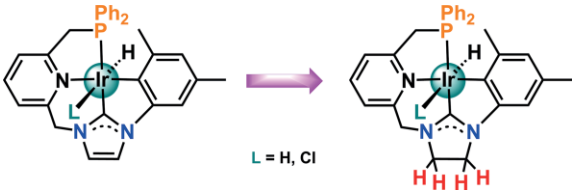

Ir complexes based on metalated CNP ligands containing either imidazolin-2-ylidene or imidazolidin-2-ylidene donors have been prepared, and their structure, photophysical properties, and reactivity towards bases and H_2 have been compared. These studies allow to propose imidazolidin-2-ylidenes as new side donors in the design of proton-responsive lutidine-derived ligands.

doi.org/10.1002/ejic.202000681